

Streamer Mechanism and Main Stroke in the Filamentary Spark Breakdown in Air as Revealed by Photomultipliers and Fast Oscilloscopic Techniques*

GILBERT G. HUDSON† AND LEONARD B. LOEB

Department of Physics, University of California, Berkeley, California

(Received June 1, 1960; revised manuscript received January 3, 1961)

A study has been made of the development of the luminosity in the transition from a corona or a Townsend predischARGE to a filamentary spark in atmospheric air for a wide range of gap geometry extending from a positive needle point-to-plane gap to large sphere-to-plane gaps very close to the parallel plate case. Two photomultipliers viewed thin slices of the gap perpendicular to its axis; the one fixed near the anode triggered the Tektronix 517 oscilloscope and the other, which could be moved parallel to the gap axis, provided the signal for display. From the oscillograms, cross plots of the developing spatial distribution of luminosity across the gap were obtained for a number of gaps. It was found that, in general, a primary and a secondary dendrite, and even a tertiary, in some cases, develop out from the anode to the cathode at high speeds and prepare the way for the growth of the main stroke. In divergent fields the primary dendrite consists of a number of simultaneous streamer filaments which, in all cases, cross to the cathode, while the branch streamers of the secondary

dendrite slow down in midgap and even fail to reach the cathode in the longer gaps. There are several sets of primary-secondary dendrites before each main stroke, in longer point-to-plane gaps, with about 200 μ sec between sets, and about 1 μ sec between the last set and the main stroke. While in the case of large sphere-to-plane gaps it was not possible to tell whether a dendrite consists of one or of several streamers, a primary (close to the cathode) and a secondary pulse can be observed in the longer gaps. With short gaps which are very close to the parallel plate case, only a secondary gap can be seen, and below about 1.0 to 1.3 cm a dendrite or streamer could not be resolved from the main stroke rise with the present equipment. In a few sphere-to-plane gaps, oscillograms and cross plots were obtained which show the development of the main stroke as its toe crosses from the anode to within about 0.5 cm of the cathode, at which position the luminosity distribution of the fully developed main stroke shows a trough, with a maximum near the anode and a rise toward the cathode.

INTRODUCTION

THAT streamers, or what might be referred to as dendrites, at least for point-to-plane gaps, play an important part in the development of the filamentary spark in air now appears well established by well-coordinated observations using four different observational techniques in several laboratories over the years from 1935 on.^{1,2} There is also evidence that a streamer-like process occurs in some other gases when impurities are present. Some common misunderstandings can be avoided if a careful distinction is made between the terms *breakdown* and *spark breakdown*. The well-known filamentary spark discharge, or spark breakdown, in gases at pressures above tens of mm of Hg is one of a group of transient, irreversible, and very fast transitions from a low-order predischARGE current to what, given proper external circuitry, would become a power arc. The filamentary spark, except at high, short impulse overvoltage, is now recognized as being preceded by a low-order self-sustaining discharge.³ These lower order discharges are at times nearly imperceptible and at other times obvious as a Townsend glow discharge in uniform fields or as corona-like breakdowns in nonuniform fields. With the very high impulse fields in overvolted gaps the predischARGE is not necessary. The *breakdown thresholds* of *predischARGES* are governed by the Townsend threshold

criterion and in most cases these breakdowns are reversible processes with relatively long formative time lags.³ In contrast, the spark-like transitions appear when, as a result of the antecedent predischARGE current, alterations in the gap, by space-charge accumulations, by changes in the state of the cathode or of the gas itself, lead to the *sudden* creation of localized, excessively high space-charge densities. Such densities create fields that cannot be dissipated sufficiently rapidly by the normal diffusion-governed charge movements.⁴ Such fields sweep across the gap at high velocities augmenting charge distribution until the arc can continue to grow by the more normal processes to its steady-state value. In particular the filamentary spark will develop whenever by geometry, the imposed field, or by space-charge buildup in uniform fields, the electron avalanches reach a certain magnitude of charge density at the anode, or in midgap.¹ This magnitude must be such that, aided by adequate photoelectric ionization in the gas near the space-charge augmented field, a *self-propagating streamer* or *dendrite* can proceed to cross the gap at high speed.⁵ The word "streamer" is being reserved for a *single* luminous filament, while the term "dendrite" is introduced here to denote a more or less tree-like configuration of a large or small number of streamers which start at the electrode as either separate filaments or as a single trunk which then develops into multiple streamers by branching (mostly in regions of highly divergent electric field). These multiple or branch streamers propagate across the gap together and, in the cases observed here for air, cross a section perpendicular to the gap axis

* This study has been supported by grants from the Office of Naval Research and from the Research Corporation.

† Now at Kyungpook National University, Taegu, Korea.

¹ L. B. Loeb, in *Encyclopedia of Physics*, edited by S. Flügge (Springer-Verlag, Berlin, 1956), Vol. 22, p. 484 ff; H. Raether, *Ergeb. exakt. Naturw.* 22, 73 (1949).

² E. Nasser, *Arch. Elektrotech.* 44, 157, 168, 455 (1959).

³ L. B. Loeb, reference 1, p. 492 ff; B. Bederson and L. H. Fisher, *Phys. Rev.* 81, 109 (1951); J. K. Vogel and H. Raether, *Z. Physik* 147, 141 (1957); H. W. Bandel, *Phys. Rev.* 95, 1177 (1954); J. K. Vogel, *Z. Physik* 148, 355 (1957).

⁴ L. B. Loeb, Report of the Third International Conference on Ionization Phenomena in Gases, Venice, Italy, June 11–15, 1957; Italian Physical Society Report, October, 1957 (unpublished), pp. 646–674.

⁵ L. B. Loeb and R. A. Wijsman, *J. Appl. Phys.* 19, 797 (1948).

so nearly simultaneously that the light signal at the PM⁶ viewing such a section cannot be distinguished from the signal due to a single "equivalent streamer." The term dendrite may also be used in a general sense to include the limiting case of a single streamer. The streamers making up a dendrite, or a temporal succession of dendrites, prepare the way for the main stroke, which follows the last of them after an interval which varies with geometry over a range from 1 or 2 μ sec down to some tens of $m\mu$ sec.

The misunderstandings earlier alluded to come from the circumstance that in the uniform field gaps usually studied the positive space-charge buildup by the antecedent Townsend discharge generally increases the avalanche size, by virtue of a well-established theorem,⁷ leading to a filamentary spark transition by anode streamer or dendrite action. Thus the threshold for the common filamentary spark *appears to coincide with the lower threshold of the Townsend breakdown*. In fact, there is only a small difference of from 4 to 6% overvoltage needed above the Townsend threshold for the direct streamer or dendrite breakdown in air, as recently shown.⁸ In relatively pure argon gas the thresholds differ by more nearly 100%.⁹ However, very slightly above the threshold for a self-sustaining Townsend discharge the space charge in both gases leads to a dendrite breakdown, as suggested for air by the oscillographic studies of Bandel³ and Kluckow.¹⁰ In air at 760 mm and 20°C a streamer or dendrite starts from the anode when the avalanche creates some 10^8 or more electrons, as shown by Loeb, Raether,¹¹ and recently more elegantly by Nasser.²

The streamer mechanism was first observed in a Wilson cloud chamber by Raether in 1935.¹ It was independently observed by Loeb and his students with visual, electrical, and oscillographic techniques using the positive-point corona from 1936 on.¹ Some early, very significant observations were made on impulse breakdown by Allibone and Meek¹² with moving film camera, and later by Saxe and Meek¹² with a PM. Most recently Nasser² has used the Lichtenberg figures on a photographic film in a plane normal to the point axis in point-to-plane geometry to study streamer branching, tip potentials, tip velocities, and to estimate critical avalanche size. The theory of streamer advance has been

developed by Meek,¹³ by Raether,¹³ and more recently including photoionization by Loeb and Wijsman.⁵ The availability of ultrafast oscilloscopes and sensitive photomultiplier tubes enabled first English¹⁴ at Chalk River and later Amin¹⁵ to achieve a temporal resolution of the electrical and luminous pulses due to preonset corona streamers. With access to the use of a 517 Tektronix oscilloscope of 7×10^{-9} sec risetime, it became feasible¹⁶ to make the observations to be reported here. This technique has since been extended to relatively pure, and to very pure argon gas by Huang and by Westberg, respectively. In this method the objective is to observe and study the progress of any streamers or dendrites which cross the gap and the growth of the spark channel at spark threshold with steady, carefully stabilized high potentials with the highest time resolution possible.

The task undertaken¹⁶ was to observe streamer or dendrite growth by viewing the gap with two photomultipliers with slits 2 cm long usually placed perpendicular to the axis of the gap. Analysis was carried out for a whole series of gaps ranging from needle point-to-plane, with gap lengths of 1 to 5 cm, to points of increasing radius opposite planes, and extending to spheres of 15-cm radius opposite planes with gaps from 1 to 9 cm in length. In all cases atmospheric air at 760-mm pressure around 20°C at about 60% humidity was studied.

FAST PHOTOMULTIPLIER TECHNIQUES

A schematic diagram of the apparatus is shown in Fig. 1. High, steady potentials from a stabilized high-potential rectifier circuit proposed by H. J. White, and similar to that designed by him and used by Fisher³ in spark lag studies, was used for work up to 74 kv. This gave a potential stable to better than 0.1%, as shown by potential measurements made with two 50-megohm wire-wound Taylor resistor stacks in series with a dial resistor box to form a potential divider, and with an L & N type *K* potentiometer to read the emf. A 70-megohm isolating resistor was used. For the breakdown at higher potentials with the longer sphere-to-plane gaps, a demonstration-type Van de Graaff generator driven by an air turbine motor was used. Sufficient charge to give a main stroke was stored on a piece of RG-8/U coaxial cable with both ends connected directly to the anode; the usual capacity was 150 pf. In the case of the work with the Van de Graaff generator the capacity of the high-voltage terminal (about 35 pf) was increased to about 135 pf by using a piece of RG-17/U cable which had had insulating oil forced into the space surrounding the central conductor by N₂ at up to 2000

⁶ The symbols PM and CRO will be used for the terms photomultiplier and cathode-ray oscilloscope, respectively.

⁷ A. von Engel and M. Steenbeck, *Elektrische Gasentladungen* (Verlag Julius Springer, Berlin, 1934), Vol. 2, p. 51 ff and p. 184; R. N. Varney, H. J. White, L. B. Loeb, and D. Q. Posin, *Phys. Rev.* **48**, 818 (1935); R. W. Crowe, J. K. Bragg, and V. G. Thomas, *Phys. Rev.* **96**, 10 (1954); A. L. Ward, *Phys. Rev.* **112**, 1852 (1958).

⁸ W. Köhrmann, *Z. angew. Phys.* **7**, 183 (1955).

⁹ G. A. Kachickas and L. H. Fisher, *Phys. Rev.* **88**, 878 (1952).

¹⁰ R. Kluckow, *Z. Physik* **148**, 564 (1957); J. K. Vogel, *Z. Physik* **148**, 355 (1957).

¹¹ H. Raether and J. Pfaue, *Z. Physik* **153**, 523 (1959); K. Richter, *Z. Physik* **158**, 312 (1960).

¹² T. E. Allibone and J. M. Meek, *Proc. Roy. Soc. (London)* **A166**, 97 (1938); **A169**, 246 (1938). R. F. Saxe and J. M. Meek, *Nature* **162**, 263 (1948), and *Brit. Elect. and Allied Ind. Res. Assoc., Reports, Ref. L/T* 183 (1947).

¹³ J. M. Meek, *Phys. Rev.* **57**, 722 (1940); H. Raether, *Z. Physik* **117**, 375, 524 (1941). See also L. B. Loeb, Office of Naval Research Technical Report, July, 1954 (unpublished), p. 74 ff.

¹⁴ W. N. English, *Phys. Rev.* **77**, 850 (1950).

¹⁵ M. R. Amin, *J. Appl. Phys.* **25**, 358 (1954).

¹⁶ G. G. Hudson, doctoral dissertation, University of California, 1957 (unpublished).

psi. The anodes consisted of a fine steel needle, platinum wires with hemispherical or sometimes slightly ellipsoidal ends. Ni wires and rods, spheres of brass, copper, and chromium-plated brass were also used. The anode tip radius varied from that of needle points up to 0.62-cm radius. For the spheres r ranged from 1.9 cm to 6.35 cm, and for the more nearly uniform field geometry larger spheres of copper up to 15-cm radius were used against planes. The small point electrodes were polished with rouge or tin oxide and wiped dust free with a clean cloth. Larger rods and spheres were buffed and cleaned with solvents. The large plane brass cathode of 12.8-cm diameter used with the smaller anodes was grounded and mounted in a large grounded metal box, together with the anode, gap condenser, and isolating resistor (Fig. 1). The gap length was varied by moving the anode holder or the cathode vertically. The inside of the top of the large (four-foot cubical) duraluminum shielding box used with the Van de Graaff generator served as the anode, and δ was varied by moving the generator vertically. The *trigger* PM, with suitable optics and viewing slit, was mounted so as to observe the space near the anode tip. It could be moved by rack and pinion to other points across the gap but was usually kept near the anode. The *signal* PM, with its optics, was moved by a calibrated screw and by a rack and pinion in the vertical and horizontal directions, respectively. Its position could be read to about 0.2 mm. It could be placed at any distance x below the trigger photomultiplier to view the light of the advancing streamer tips (whether a single streamer or a dendrite) as they cross the gap. To prevent electrical pickup, the PM unit had to be kept outside the shielding box. When the smaller shielding box was in use two achromatic lenses with $f_1=18$ cm and $f_2=9.5$ cm and of 2.3-cm diameter were employed. The slit was in the focal plane of the second lens. The first lens was adjusted so that its focal point was on the gap axis. With the larger shielding box only one lens was used. For the sphere of $r=6.4$ cm with $\delta=6.4$ cm, values of $f=18$, $u=33$, and $v=39.5$ cm were taken, where u and v are the object and image distances, respectively. For the larger spheres, values of $f=9.5$, $u=63.2$, $v=11.5$, and $2S=0.7$ cm were employed. ($2S$ is the height of the lens aperture.) The signal photomultiplier included a horizontal and vertical slit at S in Fig. 1. Thus, openings V and H of the horizontal and vertical slits could be varied from 0 to 8 and 0 to 23 mm, respectively, by means of graduated knobs. Generally for study of streamer or dendrite crossing V was set at from 0.1 to 0.5 mm and H was at its maximum. For off axis studies V was increased and H reduced to a small value or else both V and H were reduced to form a small square aperture. The 1P28 signal PM was just behind the slits and the photocathode had projected dimensions of 8 and 24 mm with the long side horizontal. The center of the cathode was 1.2 cm behind the slit. A simple shutter was mounted just behind the slits. A series tube regulated selenium rectifier circuit was used

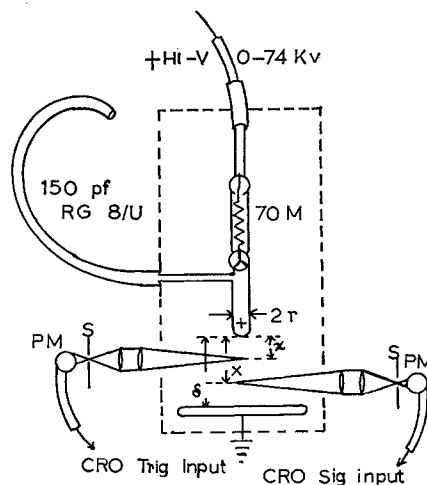


FIG. 1. Schematic diagram of apparatus.

to give the potentials of from 450 to 1500 volts applied to the PM. This supply voltage usually went directly to the trigger photomultiplier, but a potentiometer was inserted ahead of the signal photomultiplier to vary its voltage independently.

The signal from each PM was transmitted to the CRO⁶ by a 3-foot length of 170-ohm beaded coaxial cable. This matched the input impedance of the CRO which then also served as the anode load impedance. A second shielding braid was placed over each cable. In the case of the signal PM this was part of a complete outer shield that enclosed the unit and was isolated from the inner shield except where both were connected to the CRO. This double shielding, together with the complete enclosure of the gap and adjacent circuit components R_L and C_G in a metal box, was necessary to reduce the very troublesome electrical pickup that results from the spark. Although the pickup was not completely eliminated until near the end of the study, it was reduced to where it appeared only at the time of the main stroke, which gave a large signal. The streamer or dendrite pulses shown here were not affected by pickup.

The proper interpretation of the oscillograms requires an understanding of the way in which a luminous "space wave," i.e., a moving, time-varying distribution of luminosity in the gap, is transformed into the trace on the screen of the CRO. Ideally the PM should receive light from an infinitesimally thin sheet perpendicular to the gap axis. This light signal, or ideal "time wave," is then converted into an electrical signal and should be amplified by the PM and the amplifiers of the CRO and finally displayed on the CRO screen without distortion. A set of such oscillograms, each taken for a different value of x , could then be used to obtain, by cross-plotting, a corresponding set of luminosity-distance curves with t as a parameter. Such cross-plots would show the changing shape and motion of the space wave as it crosses the gap. A graph of x vs t for corresponding

points (such as the toe, a peak, or a minimum point) on these cross-plotted space waves would yield the speed as a function of x (or of t) by differentiation. The correct $x-t$ plot for the toe, or other zero point of the space wave can also be obtained directly from the zero points on the oscillograms. This is not possible for the *peak* of the space wave, since this spatial maximum is generally at a point in the gap different from that point which is experiencing a temporal maximum at the same instant. This can be visualized by studying a three-dimensional, luminosity-distance-time figure. The intersections of this surface with constant x and constant t planes are the time waves and the space waves, respectively.

The actual time waves displayed on the CRO will differ some from the ideal, due to limitations in the optical and electronic systems. The PM actually receives light from a double wedge-shaped region, the "edge" of which is the optical image of the slit at the PM. This edge thickness can be made sufficiently small by reducing the opening, V , of this slit. For points at a distance z from the $x-y$ plane the wedge thickness depends mainly on the focal length of the lens and the x dimension of its aperture. (The origin of the rectangular coordinate system is at the anode tip; the x axis coincides with the gap axis, the z axis is parallel to the axis of the PM telescope, and the y axis is horizontal and perpendicular to the telescope axis.) Mathematical analysis shows that the light flux, L , entering the PM due to a luminous filament of constant and uniform intensity at the distance z from the $x-y$ plane, will vary by about $\pm 15\%$ from L_0 , the value at $z=0$, when z covers the ranges (1) $z=-3$ to $+3$ cm, (2) $z=-4$ to $+6$ cm, and (3) $z=-8$ to $+10$ cm for the optical systems used, respectively, with (1) the small shielding box and point anodes, (2) the large shielding box and the sphere with $r=6.4$ cm, and (3) the large box and all other spheres. However, the total light flux for a bundle of such line sources, or for a cylindrical luminous volume lying within these ranges of z will be very nearly the same as for a single filament on the x axis and which has the same intensity per unit length. This means that, by means of the trace on the CRO, one cannot distinguish between a bundle of simultaneous streamers, a luminous channel of large diameter, and a single filamentary streamer (though in the last case the amplitude varies with z to some extent). To determine the distribution in the $y-z$ plane, it is necessary to use a vertical slit or a very small square aperture at the PM and to scan the gap horizontally. It should be noted that the concept of depth of focus used in photography cannot be employed here.

When actual moving space waves are considered, it is seen that the toe of a streamer not in the $x-y$ plane enters the double wedge earlier, and its heel leaves later than a simultaneous streamer in the $x-y$ plane. As a result the rise of the corresponding trace on the CRO will be somewhat earlier than it should and its return to zero will be somewhat late. In addition the dip between

two maxima that follow very closely in time will be reduced. The resolving power of the electronic system is limited by the rise time τ_R of the CRO. Even though the light time wave at the photocathode of the PM may rise (or fall) more quickly, the CRO trace cannot rise in a time less than τ_R . Accurate cross plots cannot be made from portions of an oscillogram subject to this limitation.

EXPERIMENTAL OBSERVATIONS

The investigation began with fine point-to-plane geometry, the anode radius increasing progressively to that of a 31-cm diameter sphere as the study proceeded. Figure 2 shows the traces for a needle point *below* spark breakdown in a 5-cm long gap for the first 2 cm of the gap taken by Amin and Hudson. Here the streamer process is clearly seen to be composed of a *fast primary streamer* or *dendrite* and a slower secondary which are not at first resolved. The primary emerges and increases in amplitude as it proceeds at high speed into the gap. The repeated primary traces show some scatter after traversing about 40% of the gap length and show a cessation of advance shortly beyond. The initially very *bright but slower secondary dendrites* at first mask the primaries but attenuate rapidly, being barely perceptible at 0.33 cm from the anode. The oscillograms of Fig. 2 are due to ten or more repeated sweeps. The nearly complete overlapping of these traces out as far as 0.93 cm (frame omitted from Fig. 2) indicates the remarkable uniformity of the primary dendrite process over this distance. But there is considerable jitter in time as the primary reaches $x=1.93$ cm. The low-amplitude oscillations immediately following the primary pulse are due to electrical noise that had not then been eliminated, but was later.

In order to deal only with dendrites that lead to breakdown and to eliminate those which do not and would only complicate the record, the gap length δ was

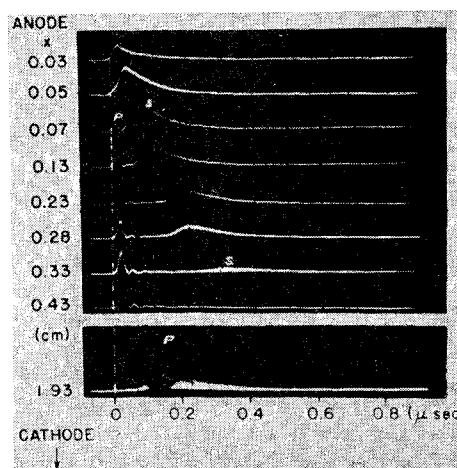
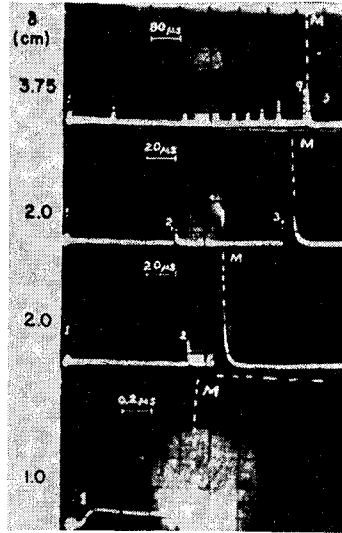


Fig. 2. CRO traces showing primary and secondary dendrites below breakdown for a needle point with $\delta=5$ cm.

FIG. 3. Oscillograms, taken at slow sweep speeds, of the succession of dendrite sets preceding a single main stroke for several gap lengths with the same point (tip $r=0.04$ cm). Primaries and secondaries are unresolved.



shortened and the anode radius r was increased, that is, δ/r was made less than 160 in air at 760 mm.¹⁷ Under this condition dendrites, other than those at corona onset, occur only as part of the breakdown mechanism. A number of point-to-plane gaps for which $\delta/r < 160$ were included in this study. Values of r ranged from $r=0.025$ to 0.62 cm, and gap length was varied from $\delta=1$ to 3.75 cm. In most of these cases there is a steady corona glow on the anode surface below the sparking voltage; otherwise there is undoubtedly a Townsend predischARGE which prepares the way for the streamer or dendrite process. All previous investigations with less time resolution had led to the expectation that there was just a single straight or branched streamer crossing the gap before what Loeb initially called the *return stroke*, but which is now best called the *main stroke* (i.e., the incipient arc phase). In this range of gap geometry the main stroke is preceded by one or more sets of dendrites separated by intervals from 20 to over $200 \mu\text{sec}$. Each set consists of a primary and a secondary dendrite, and the number of sets, n , depends on the geometry. For example, for an anode of tip $r \approx 0.04$ cm $n=9$ for $\delta=3.75$ cm, and $n=1$ for $\delta=1.0$ cm, as seen in Fig. 3, the oscillograms of which were obtained with a Tektronix 511 A CRO. Because of the long rise time and low writing speed of this instrument, it was necessary to increase the RC of the PM output circuit. As a result each pip on one of the traces in Fig. 3 represents one set of primary and secondary dendrites which, however, are unresolved. The rise point of the main stroke, M , is shown satisfactorily, but its shape is distorted due to the rise time limitation and to overloading of the CRO amplifier. For this range of geometry all primaries cross the gap. The secondaries cross in the shorter gaps but they become too feeble to be seen in the cathode region of the longer gaps. There could be a lower order current due to electron multiplication and

with lower relative light output. Perhaps this could extend the space charge of the secondary to the cathode, provided there is time before the rise of the main stroke. In the point-to-plane gaps reported on here (except for the case of $r=0.1$ cm and $\delta=1.7$ cm), the main stroke rise follows the primary of the last set in something like $1 \mu\text{sec}$.

For a slightly smaller point with $r=0.04$ and $\delta=3.0$ cm Fig. 4 shows the primary and secondary pulses clearly resolved. Here superposed sweeps record events taking place when there were about 7 dendrite sets preceding a single main stroke, which is off scale to the right. Especially at $x=0.3$ cm secondaries show a definite progression in arrival time and amplitude in each breakdown sequence, but the direction of this trend is not indicated. For $x=0.8$ to about 1.9 cm some sets do not include a secondary, and beyond $x \approx 1.9$ cm no secondary pulse is seen. The main stroke follows within 0.3 to $1.7 \mu\text{sec}$ after the last primary.

A rather unusual case is presented in Fig. 5 for a gap with $r=0.1$ cm. The first trace shows the first streamer or dendrite set, which crosses the entire gap but with such low relative intensity that it is difficult to tell whether it includes both a primary and a secondary. Its speed is low—about the same as that of the secondary of the second set. Though the intensity of the final primary increases as it crosses the gap, it travels with a rather constant speed of 1 to 2×10^8 cm/sec, while the secondary toe slows down markedly near the cathode and has an average speed of $\sim 2 \times 10^7$ cm/sec. Near the cathode the interval between the final secondary and the main stroke is so short that the secondary appears as a shoulder on the rise of the main stroke, which, of course, appears highly distorted in Fig. 5. No significance can be attached to the variation with x of the time of

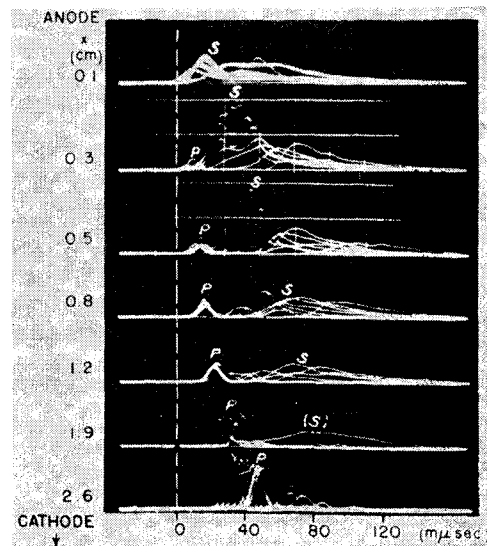


FIG. 4. Superimposed traces at varying x of the seven, or so, primary-secondary dendrite sets preceding a single main stroke. (Two main strokes at $x=2.6$ cm.) $r=0.04$ cm, $\delta=3.0$ cm.

¹⁷ H. W. Bandel, Phys. Rev. 84, 92 (1951).

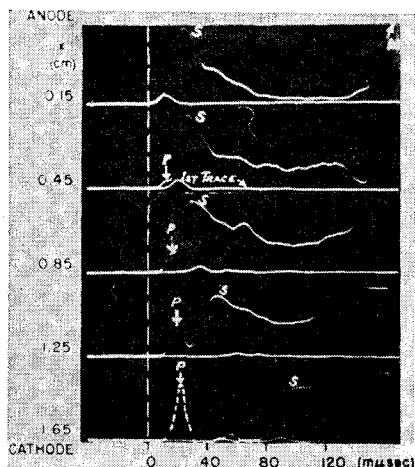


FIG. 5. Oscillograms of the two dendrite sets preceding the main stroke, the rise of which appears at the right on the second trace. $r=0.1$ cm, $\delta=1.7$ cm.

rise of the main stroke in Fig. 5 as this time varies considerably from spark to spark at any given x for this gap.

For a gap with $r=0.62$ cm and $\delta=1.5$ cm there is no corona below breakdown and only one streamer set precedes each main stroke, which follows the primary in about 1 μ sec, on the average. Both primary and secondary reach the cathode. If δ is increased to 2.5 cm, corona appears on the point surface in a narrow range of voltage, and two streamer sets precede each main stroke. The intervals from the first and second primaries to the main stroke are, respectively, 100–200 μ sec and 1–2 μ sec. The primaries cross to the cathode, but the secondary luminosity fades out at $x \approx 2$ cm.

With this same anode ($r=0.62$ cm) and $\delta=3.0$ cm it was possible, under special conditions, to make both visual and photographic observations of what were essentially breakdown dendrites in the absence of the blinding main stroke. This apparently came about because a slight cusp remained at the tip of the electrode after the polishing operation. After this was removed in later repolishing, the dendrite was always followed by the main stroke. In the absence of the main stroke perhaps 30–40 faintly luminous filaments could be seen with the aid of the telemicroscope in the cathode portion of the gap at the same time that one primary pulse appeared on the CRO. These filaments were shown to constitute a primary dendrite by the fact that only a primary pulse appeared on the CRO trace in this region ($x \geq 2$ cm). Though the oscillograms showed considerable fine structure, possibly indicating additional primaries reaching the particular value of x at various times, the large initial, or principal, pulse was due to the simultaneous streamers forming one developing dendrite lying within a volume having a diameter of at least 1.6 cm at $x=1.9$ cm. This was demonstrated by reducing H , the horizontal dimension of the slit at the PM, and also by scanning the gap horizontally with a small square aperture instead of a slit. These streamers in such a

dendrite could be followed all the way to the cathode, where they terminated in bright spots, which are probably due to the photoelectrons that are produced by photons from the streamer tip and then produce electron multiplication and excitation in the high electric field between the streamer tip and the cathode. These individual streamer filaments, which are a fraction of a mm in diameter, can be seen, though faintly, on the original negative of Fig. 6(a). Only a small number of them are recorded on this negative, due to the small depth of focus (2 mm) of the camera lens. In the reproduction of this figure only the image of three successive secondary dendrites can be seen. These are identified as secondaries by means of the CRO. They are seen to be straight for about the first 0.3 cm, beyond which branching occurs. Beyond $x \approx 2$ cm the secondaries are too feeble to produce a deflection on the CRO traces observed. Acoustically the development of one of these dendrites is quite noisy, though not as loud as a main stroke. Figure 6(b) is a time exposure produced by about 40 successive dendrites. Individual streamer filaments cannot be seen, but it is clear that the primaries cross the gap and produce cathode spots. A somewhat similar time exposure due to streamers from a needle point very close to breakdown was made by Kip,¹⁸ but at that time it was not possible to tell whether a pulse on the CRO was due to a single streamer or to a dendrite. Streamer branching in a positive point-to-plane gap with impulse voltage and high overvoltage was photographed by Gorrill¹⁸ in a cloud chamber. One of his pictures, which probably records a secondary dendrite, is shown in Fig. 7. Similar cloud track photographs of the branching of streamers from a point had been made in Raether's earliest studies, but were not then interpretable. In the work of Saxe and Meek¹² a "corona head" was observed to precede the advancing leader in the impulse breakdown of long gaps. It is conceivable that this may have been due to multiple and branched primary streamers, that is, to a rapid succession of primary dendrites emanating at high speed from the more slowly advancing leader tip. The leader stroke itself, with a maximum speed varying from 10^7 to 4×10^7 cm/sec, may be similar to the secondary streamer or dendrite observed here and which has speeds of the same order of magnitude in divergent fields. The

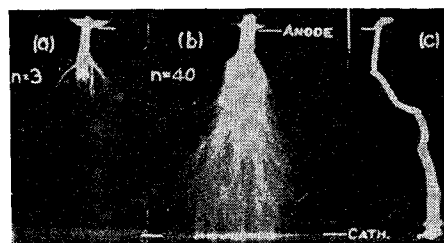


FIG. 6. Still photograph under unique geometry, showing streamers just at breakdown and resulting spark at right.

¹⁸ A. F. Kip, Phys. Rev. **55**, 549 (1939); W. S. Gorrill, doctoral dissertation, University of California, 1939 (unpublished).

leader stroke, however, does have a much larger diameter (~ 1.7 cm) than that of the secondary streamer filament. In general, branching is greatest where fields are highly divergent in point-to-plane gaps, with long gaps, and in highly overvolted impulse breakdown. They spread least in short, uniform field gaps where the observed spark channels are short and straight. The photograph in Fig. 6(c) shows a single spark in the present gap, which is straight for the same distance as the intense, straight secondaries in Fig. 6(a). It may be that the main stroke follows the path of the most strongly developed secondary.

The length of the secondary streamers, the branching, and the time between the first primary and main stroke are not affected by the size of the gap condenser, C_g , in the range 150 to 2000 pf. They are purely functions of the field distribution in the gap.

The existence of such branching has recently been confirmed and investigated in detail by Nasser² using the Lichtenberg figures created at the point of impact of the streamers on a photographic film placed parallel to the plate at various distances x from the anode. Here each primary streamer produces a Lichtenberg figure along the surface of the film, the maximum length of which is proportional to the potential of the streamer head at that point. He has studied these both above and below breakdown threshold with impulse potentials of short duration. The branching increases as the distance x from the anode increases. It is the greater the higher and more divergent the field. As many as 100 branches were observed near the cathode. Where primary

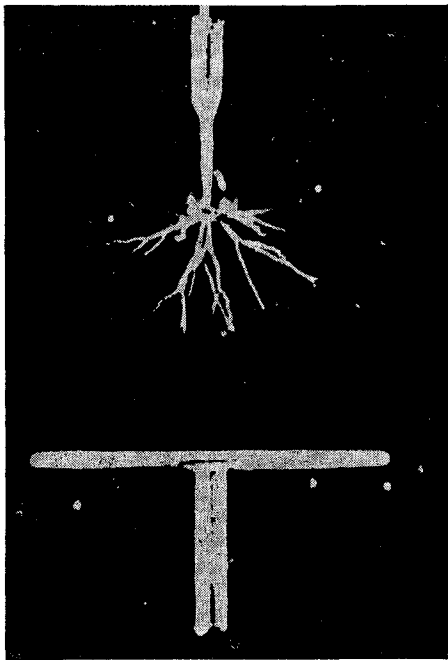


FIG. 7. An early cloud chamber photograph of branched secondary streamers in interrupted point-to-plane impulse breakdown by Gorrill.

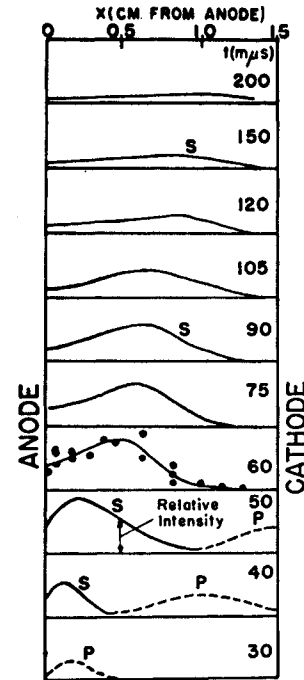


FIG. 8. Cross plots of streamer luminosity across the gap at different times in μsec , illustrating movement of primary and secondary space waves.

streamers do not cross the whole gap the photographic plate for a mm or two beyond the point where streamers end is blackened by the photons emitted from the streamer tips. This confirms Kip's¹⁸ early observations with ion currents using a screening grid over the cathode with auxiliary field.

One of the remarkable features concerning these primary streamer branches is that within the limits of resolution of the system the tips appear to advance across the gap to reach the same horizontal plane at x , at about the same time, irrespective of the value of the radial distance from the x axis. The results in this particular gap suggest that there is a dendritic structure of simultaneous streamers in other gaps where the PM reveals a rather large envelope of the streamers.

Figure 8 shows a cross plot for a gap with $r=0.62$ cm and $\delta=1.5$ cm. Here ordinates represent luminous intensity as sensed by the photomultiplier corrected for variations in gain, while abscissas correspond to the distance x , with anode to the left and cathode to the right. These are presented for different times from 30 to 200 μsec . The scatter of points read from the traces at 60 μsec gives some idea of the accuracy of cross-plotting. Later investigations gave much improved accuracy. Each point is based on the average of the five or so oscillograms on a single frame. Points were taken from a total of 22 frames for each gap. Fine structure on the oscillograms, due to delayed multiple primaries and secondaries, was ignored, so that the cross plots represent the initial or principal dendrite. The dashed lines indicate that the oscillograms, and hence the cross-plotted space waves, are not too accurate in these regions due to the limitation imposed on resolu-

tion by the CRO rise time. Since the photomultiplier integrates the light from the dendrite as it crosses a thin slice of the gap, these space waves also represent the "equivalent streamer" with the same total intensity per unit length as the actual distributed luminosity. The growth, development, and crossing of the equivalent streamer is clearly depicted.

Figure 9 gives a plot of x for the peaks against t for the primaries and secondaries taken from the cross plots of Fig. 8. Here the constant and high speed of the primary dendrite is noted. The secondary is seen to undergo a marked change in speed after traversing the first third of the gap. The primary dendrite advances with the uniform speed of about 7×10^7 cm/sec. In the first third of the gap near the anode, where there is not much branching, the secondary dendrite follows a path with high initial density of ionization and its speed is 2×10^7 cm/sec. Once the secondary branches the speed decreases to 3×10^6 cm/sec. The secondary *toe* reaches the cathode at about $t = 0.2 \mu\text{sec}$. The peak should arrive at $t = 0.33 \mu\text{sec}$ but its intensity is very low near the cathode. The main stroke rise occurs at about $1 \mu\text{sec}$. For the somewhat longer 2.5-cm gap with the same anode the primary speed is 6×10^7 cm/sec and the initial and final speeds of the secondary are 1.7×10^7 and about 4×10^6 cm/sec, respectively. As already mentioned, in this large gap the secondary becomes too feeble to be observed on the CRO trace beyond $x \approx 2$ cm, but if the secondary peak were to continue with the same speed as observed in midgap it should reach the cathode at $t \approx 1.7 \mu\text{sec}$, which lies in the middle of the observed range for the time from the last primary to the main stroke rise. Since this primary-main stroke interval agrees roughly with the time of arrival of the "extrapolated secondary peak" at the cathode for $\delta = 2.5$ cm, but definitely does not for $\delta = 1.5$ cm, it is difficult to explain this interval. It is seen that the longer the gap the lower the dendrite speeds, as might be expected.

It was decided to begin with small spheres as anodes and then to increase r and to vary the gap lengths so as

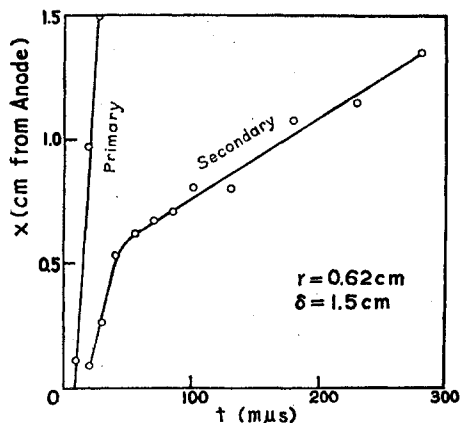


FIG. 9. Time-distance plots for primary and secondary space waves.

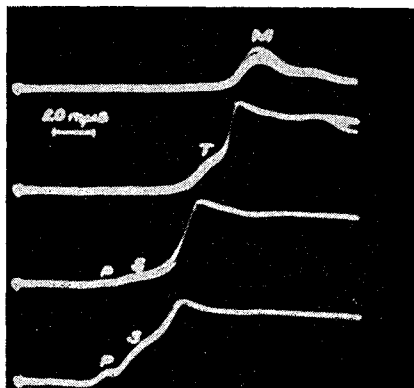


FIG. 10. Near the cathode the main stroke and tertiary, secondary, and primary pulses appear in successive frames as the PM slit width increases from top to bottom. The origin of time is the same for all frames. Sweep rate = $20 \mu\text{sec/cm}$. $r = 1.9$ cm, $\delta = 1.5$ cm.

to approach the parallel plate case and at the same time keep the sparks sufficiently localized to permit observations with photomultipliers. The electrostatic generator was used to supply the higher voltage needed for the longer gaps (and also to make it possible to eliminate pickup in the PM circuit by having all electrical components related to the gap entirely enclosed in the large shielding box), but with this device the voltage rises after each spark along some sort of a curve which approaches asymptotically the maximum attainable voltage for this machine. This means that the voltage is rising fairly rapidly as it nears the breakdown threshold for the gap under study, and that there may be considerable overvoltage, unless triggering electrons are supplied at a sufficiently high frequency. A small quantity of thoriated ore was used in all cases to provide these electrons. Very rough estimates of the overvoltage, based on the activity of thoriated, the sensitive volume and the "counting efficiency" of the gap gave values between 5.6% for the gap with $r = 1.9$ and $\delta = 1.5$ cm, and 0.006% for the case of $r = 15.5$ and $\delta = 6.0$ cm. No doubt the first figure is much too large, because when ultraviolet light was also used on this gap and the overvoltage was estimated to be of the order of 0.01% the oscillograms were unaltered. It is very easy to have so much ultraviolet incident on the cathode that, just below breakdown, the gas-amplified photoelectric current equals the charging current ($1 \mu\text{a}$) and the breakdown voltage is not reached. In addition some brief tests with pulsed voltages on point-to-plane gaps suggest that the nature of the breakdown mechanism may not be materially altered for overvoltages as high as about 10%, though the primary-main stroke interval is reduced. Another interesting observation with pulsed voltages is that the sparks are much more crooked in the cathode portion of the gap at high overvoltage. This may be due to the fact that during the application of the approach voltage, prior to the addition of the pulse voltage, there is more space charge in the gap, which

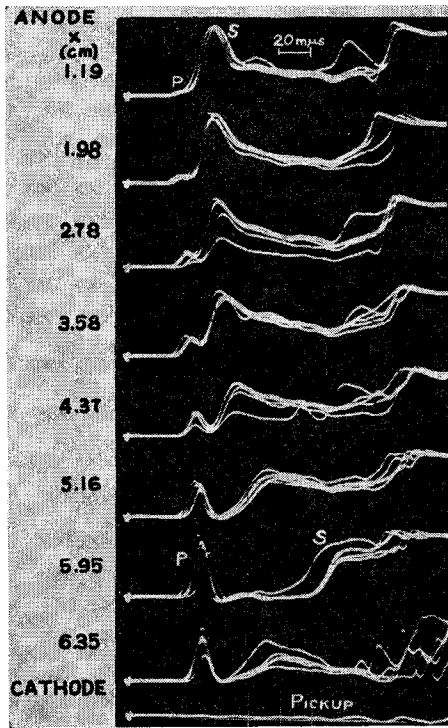


FIG. 11. The development of the single primary-secondary dendrite set preceding each main stroke for $r=6.35$ cm and $\delta=6.4$ cm. The main stroke overloads the CRO, but its rise appears at the right.

makes it easier for the main stroke, and probably the antecedent streamers or dendrites, to follow devious paths.

Since there has been difference of opinion as to whether streamers actually play a role in the development of the common filamentary spark in uniform field geometry where the pre-main stroke Townsend discharge builds up a positive ion space charge that could give rise to a streamer, it was urgent that gaps approaching as nearly as possible the uniform field geometry be investigated. Since for observation by means of photomultipliers the spark and streamer channels must be created near the x axis with a maximum radial displacement of perhaps 1 cm, actual parallel plate, or uniform field geometry could not be used. With that geometry the breakdown may occur at any chance point over the large electrode area. The nearest approach that gave axially centered breakdown was with a sphere of 31-cm diameter opposite a plane.

The first step in this approach to the parallel plate gap was made with values of $r=1.9$ and $\delta=1.5$ cm. Ultraviolet, as well as thorianite, was used to provide triggering electrons. A set of four oscillograms is shown in Fig. 10 for a position close to the cathode ($x=1.43$ cm). Pickup had been reduced to essentially zero when these oscillograms were taken near the end of the project. The relative gain increases from frame to frame beginning at the top, but without changing the voltage

on the PM so as not to shift the origin of time by altering the electron transit time in the PM. The traces in the top frame show the main stroke, M , without distortion. (The peaks in the other three frames are distorted due to overloading of the CRO amplifiers.) In the second frame a tertiary pulse, T , is observed at the toe of M . In the two lower frames the primary and secondary pulses, P and S , can be seen at the toe of T . Though oscillograms for various values of x were made for only the main stroke pulses in this gap, visual study of the

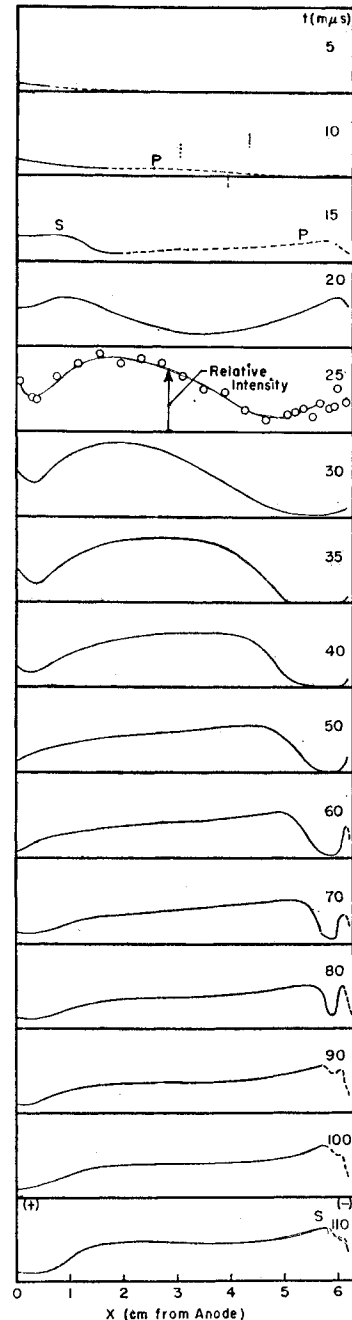


FIG. 12. Cross plots showing the luminous primary and secondary space waves from 5 to 110 mμsec, taken from oscillograms of Fig. 11.

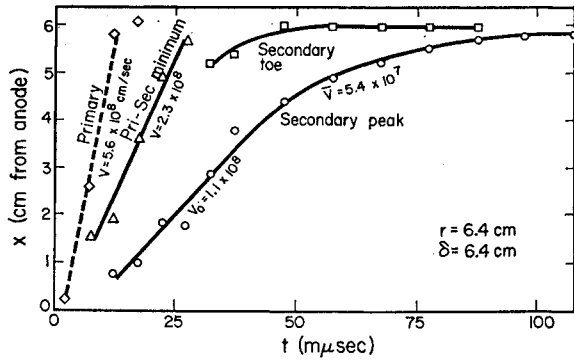


FIG. 13. Time-distance plots for space-wave features of Fig. 12.

pulses due to *P*, *S*, and *T* showed that the primary could be resolved only near the cathode, the secondary throughout the gap, and the tertiary beyond $x = 0.79$ cm. Even though the speeds of *P* and *S* are so high that the direction of motion could not be determined by visual study of the traces on the CRO, these are no doubt primary and secondary dendrites, since the pulses are similar to those seen in longer gaps where the motions are definitely revealed by the cross plots, and also since the time scale of the breakdown mechanism tends to become compressed as r increases and δ decreases. The oscillograms photographed for the main stroke show that the toe advances at about 6×10^7 cm/sec out to $x \approx 1.2$ cm, where it is met by the cathode luminosity. Cross plots, if made, would show that the main stroke space wave has a maximum at $x \approx 0.5$ cm and a trough at $x \approx 1.1$ cm.

Oscillograms for the case of $r = 6.35$ and $\delta = 6.4$ cm are shown in Fig. 11. Each of the five traces shown on any one frame records the single set of primary and secondary pulses which precedes each main stroke. The rise of the main stroke appears at the right, but the rest of this pulse is distorted. The development of the space wave with time is seen in the cross plots of Fig. 12. The speeds of the various points on the space wave are derived from the $x-t$ plots of Fig. 13 and are given on that figure; they range from a constant value of about 5.6×10^8 cm/sec for the primary to an average speed of about 5.4×10^7 cm/sec for the secondary peak. It should be noted that all speeds increase as the gaps approach the uniform field condition with higher fields out in the gap. Neither the toe nor the peak of the secondary shows any advance beyond $x \approx 6$ cm, though, during the interval $t = 60$ to 90 mμsec, there is a rise in luminosity within 0.5 cm of the cathode. Possibly there is also a narrow dark space next to the cathode, though the shape of the space wave in this region is not absolutely certain, as indicated by the dashed portions of the cross plots in Fig. 12. Except for the narrow region near the cathode the cross plots are reasonably accurate, as suggested by the plotted points at $t = 25$ mμsec in Fig. 12.

For the spheres with $r = 6.35$, 10.2, and 15.5 cm commercially-made copper float balls were used. Though the

surfaces of these showed noticeable variations in curvature, the portions of the surfaces used in the sparking area were sufficiently uniform for the purposes of this study.

For the largest sphere ($r = 15.5$ cm) and a gap $\delta = 1.65$ cm the oscillograms of Fig. 14 show what may be considered a streamer or dendrite, *S*, at the toe of the main stroke in the cathode half of the gap. This can probably be called a secondary dendrite, since it comes just before the main stroke, even though a primary pulse cannot be seen in this short gap, at least with present equipment. If this secondary dendrite, or its toe, actually moves across the gap its speed is so high (perhaps greater than 6×10^8 cm/sec) that the motion is not revealed in Fig. 14. Since the main stroke peaks are distorted in this figure, it would be necessary, in order to see them correctly displayed, to look at traces, taken with reduced gain, which unfortunately cannot be shown. However, the cross plots derived from them shown in Fig. 15 exhibit a definite motion of the main stroke toe from anode toward the cathode. The average speed for the toe, as obtained from several sets of oscillograms and from the cross plots, is of the order of 6×10^7 cm/sec for the main part of its motion. Though the rise point of the main stroke is fairly constant at a given x , except at $x = 0.16$ cm, the height of the trace varies considerably

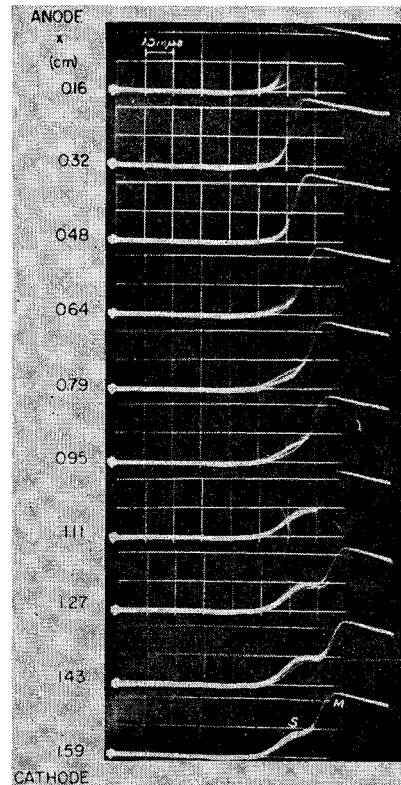


FIG. 14. CRO traces, for nearly parallel plate geometry, showing a streamer, or dendrite, in the cathode half of the gap, and the main stroke toe. (Its peak overloads the CRO.) $r = 15.5$ cm, $\delta = 1.65$ cm.

from spark to spark, and "average" traces were used to obtain the cross plots of the space wave. The main stroke peak also shows some motion until a maximum is reached at $x=0.5$ cm and $t \approx 30$ to $35 \mu\text{sec}$, after which it appears to recede toward the anode. There is also a marked minimum at $x=1.3$ cm for $t \geq 30 \mu\text{sec}$. In the cathode region the intensity rises again to an intermediate value. The dashed lines on these cross plots represent those time waves for $x=0.16$ cm which show a late rise but a higher maximum. While there is definite motion of both the toe and the peak of the main stroke, the over-all buildup of space-wave intensity throughout the gap is at least as pronounced as the motion across the gap. It appears that the total light output of the main stroke (area under the space wave) increases more rapidly after the secondary peak has reached the cathode at $t=12.5$ to $15 \mu\text{sec}$.

Sets of oscillograms for a gap with the same anode ($r=15.5$ cm) and $\delta=6.0$ cm are shown in Figs. 16 to 18. Cross plots of the developing space waves in this gap are

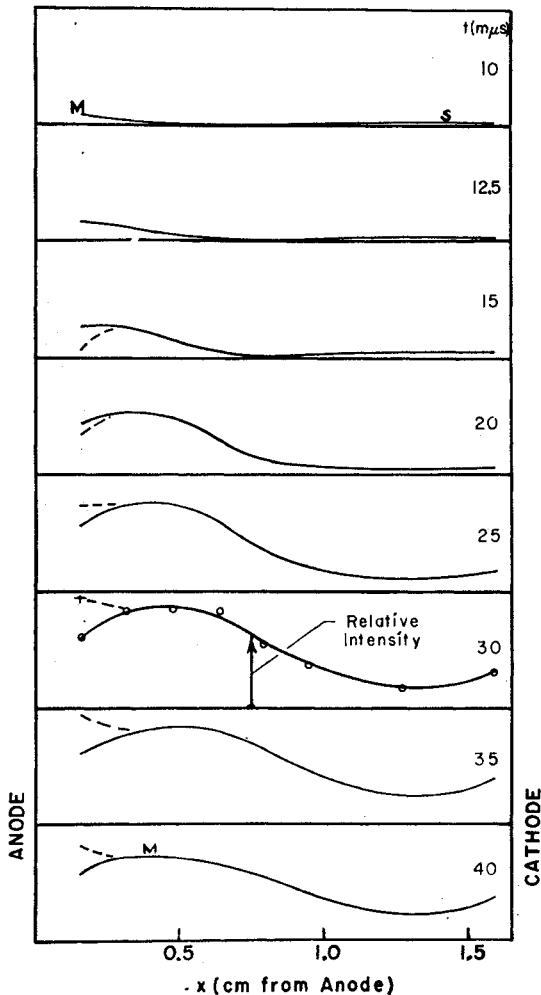


FIG. 15. Cross plots showing the main stroke space wave at successive times for $r=15.5$ cm and $\delta=1.65$ cm.

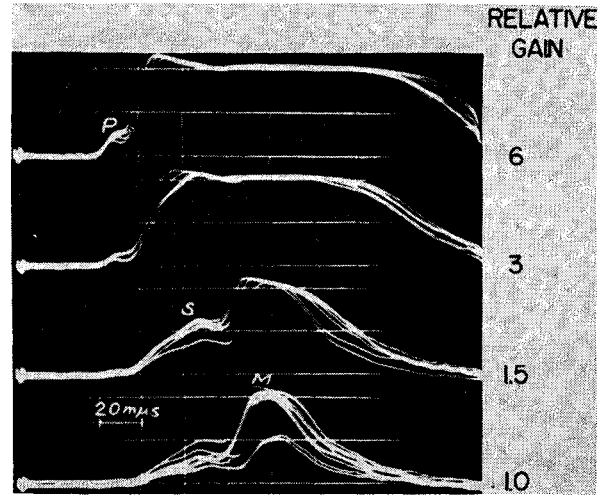


FIG. 16. Oscillograms on fast sweep at varying gains near cathode for $r=15.5$ cm and $\delta=6$ cm, showing primary, secondary, and main stroke. The origin of time was fixed as only the PM slit was varied.

presented in Figs. 19 to 21. The four frames of Fig. 16 were taken at $x \approx 5.7$ cm with varying relative gain, as indicated on the figure. In the bottom frame the main stroke, M , is already slightly distorted. The secondary, S , overloads the circuits in the two top frames. The pulse P , which is clearly seen in the two top frames and can even be detected in the two bottom frames, is probably due to a primary dendrite, even though it is not possible to see any motion of its toe in the oscillograms of Fig. 17. This primary also produces the slight rise of the space wave close to the cathode for $t=7.5$ to $12.5 \mu\text{sec}$ in Fig. 19. Nor can one see any motion of the secondary toe, except in the cathode region ($x \geq 5.4$ cm in Fig. 17) where it is resolved from the primary. This checks with the cross plots (Figs. 19 and 20), which show only a slight motion of the toe out to $t=15 \mu\text{sec}$. At $t=12.5 \mu\text{sec}$, just before the secondary toe reaches the cathode, the first sign of the secondary-main stroke minimum appears at the anode. The secondary peak shows a very definite motion across the gap (Figs. 19 to 21) at a speed of about 1.5×10^8 cm/sec for the main part of this motion. In this gap also the total light output of the main stroke begins to increase rapidly at about the time the secondary peak reaches the cathode ($t \approx 30 \mu\text{sec}$ in Fig. 20). Movement of the main stroke toe (secondary-main stroke minimum) from the anode to within 0.5 cm of the cathode is clearly revealed both in the oscillograms of Fig. 18 and in the cross-plots of Figs. 20 and 21 especially. Its speed is variable but is about 1.4×10^8 cm/sec between $x \approx 2.2$ and 5 cm. The peak of the main stroke moves out to about $x=0.7$ cm at $t=78 \mu\text{sec}$. At about this same time the space wave reaches its maximum value at all points in the gap almost simultaneously, as seen in Fig. 21, with a peak at $x \approx 0.7$ cm, a trough at $x \approx 5.5$ cm and probably a rise in intensity close to the cathode. Though this rise is in

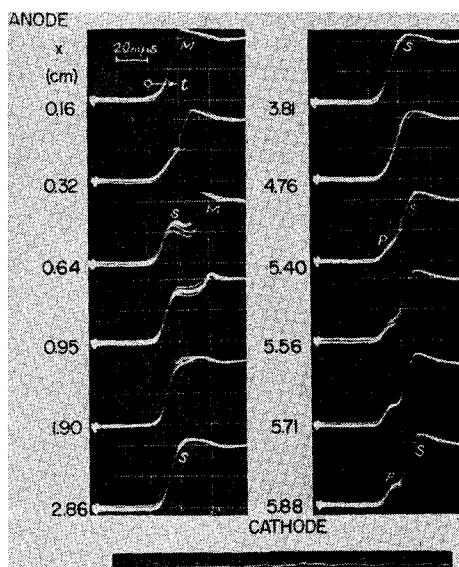


FIG. 17. CRO traces showing the primary (near the cathode), the secondary (with CRO overloaded for $x > 0.95$ cm), and the toe of the main stroke (for $x \leq 0.95$ cm). $r = 15.5$ cm, $\delta = 6$ cm. Electrical pickup on trace below.

a region where the points on the cross plots show some scatter, it is no doubt real since a similar rise appears in Fig. 15, the data for which are more accurate. It is interesting to note that, at this same time, the distances of the peak from the anode and of the trough from the cathode, are about the same as the values found with this sphere and a gap length $\delta = 1.65$ cm. The over-all growth of the luminosity distribution for both the secondary and the main stroke is as significant as their motion from the anode toward the cathode, as in previous cases.

DISCUSSION

The observations presented show that, in general, a dendrite, consisting of one or more simultaneous streamers, crosses from anode to cathode and produces the transition from the steady corona or the Townsend pre-spark discharge to the main stroke in the spark breakdown of room air at one atmosphere for the range of gap geometry studied, that is, from the positive needle point-to-plane through point- or rod-to-plane gaps of 1 to 3 cm in length, and on to positive sphere-to-plane gaps with sphere radii up to 15.5 cm and gap lengths between 1.3 and 6.4 cm (and even 9.5 cm in one case). That a Townsend predischage occurs in the gaps where no corona is observed is indicated by the results of Fisher³ and of Bandel.³ The resulting space-charge accumulation in the gap produces an increase in the field near the cathode and, in many cases, near the anode with the result that the number of electrons per avalanche is increased, whether that avalanche starts with a photoelectron produced at the cathode or in the gas. Probably there is a final rapid rise in current, as observed by Bandel, and at some point on this rise the

dendrite is initiated at the anode and progresses into the gap. In general, it soon divides into a fast primary and a slower secondary. The primary may be a kind of traveling space-charge dipole wave which carries its own high axial field ahead of its advancing positive tip and thus is able to cross the entire gap, even through the low applied fields near the cathode of point-to-plane gaps. Propagation of the primary probably depends mainly on the avalanching of electrons produced by photoionization of the gas ahead of the advancing tip, with perhaps some avalanching of electrons produced in the predischage phase and suddenly accelerated by the tip field. The fact that many successive avalanches pass axially through a fixed volume element ahead of the tip may contribute to the high speed of the primary, which is constant for a given gap but increases as the geometry is changed from the point-to-plane to the near uniform case. Values of the primary speed range from 2×10^7 to 6×10^8 cm/sec, and higher. In point-to-plane gaps the dendrite is found to consist of a number of streamers, or single filaments, which are probably the result of branching near the anode. These individual streamers cross simultaneously and produce a single, sharp primary pulse on the CRO. The extent of the branching or the multiplicity of the primary streamers could not be determined for sphere-to-plane gaps; it may be that the dendrite becomes a single streamer as the parallel plate gap is approached.

It has been suggested by Loeb⁴ that, because it acts

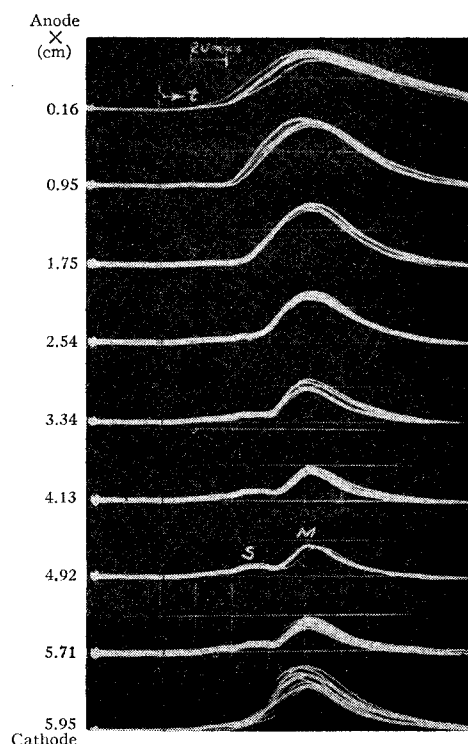


FIG. 18. Oscillograms showing secondary streamer and main stroke for $r = 15.5$ cm, $\delta = 6.0$ cm.

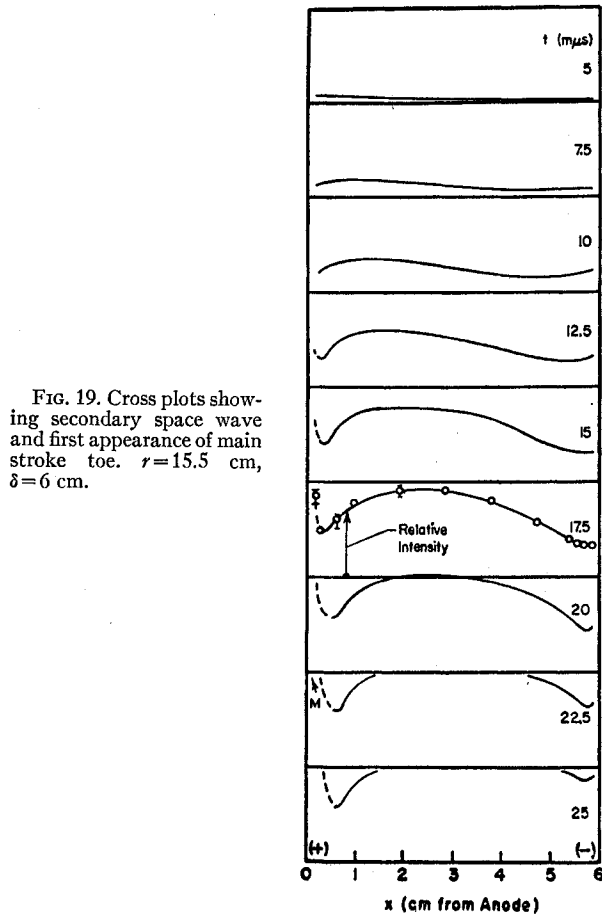


FIG. 19. Cross plots showing secondary space wave and first appearance of main stroke toe. $r=15.5$ cm, $\delta=6$ cm.

for too short a time, no one of the primary streamers produces enough ionization in its channel to permit the immediate development of the main stroke, but instead prepares the way for the secondary dendrite. Loeb has also suggested that the secondary may be initiated by an ultrafast return wave, similar to those observed by Westberg,¹⁹ and which is in turn triggered by the photoelectrons from the cathode spot evidently formed by each primary streamer. However, more evidence is needed on this point since in some cases the secondary is well under way before the primary has reached the cathode with appreciable intensity. The secondary may develop through a combination of (1) radial expansion due to photoelectrons avalanching radially inward to the primary streamer channel, as proposed by Loeb,²⁰ and (2) ionization accompanying the axial motion of the electrons in this same channel, especially after the passage of the secondary toe has begun to increase the density of ionization. An attempt to measure a difference in the diameters of the primary and secondary channels yielded a negative, though possibly not a conclusive result. That the second process may be important is indicated by the fact that the development of the

secondary evidently depends strongly on the pre-existing field distribution, since it branches and slows down markedly at a short distance from the anode, and becomes too feeble for it to be seen beyond midgap in longer point-to-plane gaps. The secondary speed also increases as the uniform field case is approached, with values ranging from 10^6 to 6×10^8 cm/sec, and greater, for the secondary toe. In addition to the axial motion the secondary also shows a pronounced rise in intensity

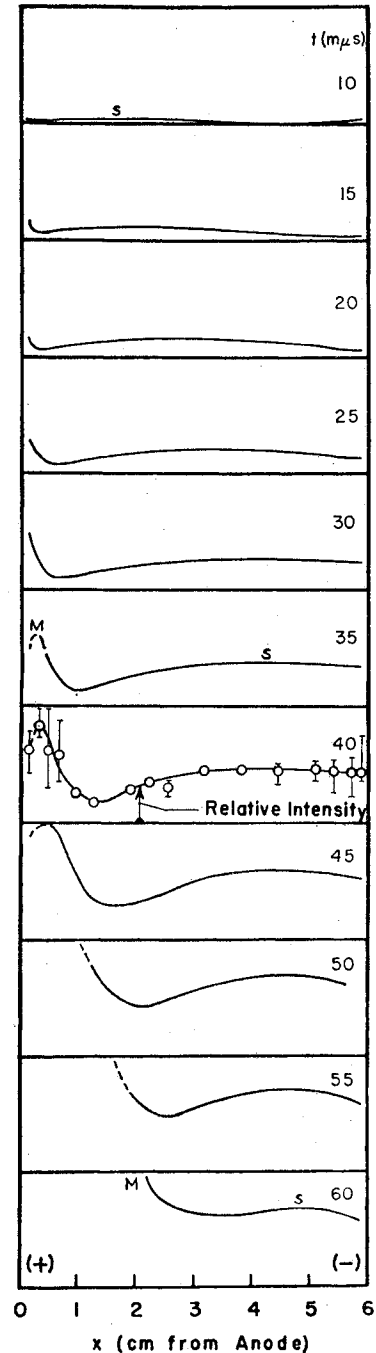


FIG. 20. Cross plots for secondary streamer and rise of main stroke, $r=15.5$ cm, $\delta=6$ cm.

¹⁹ R. G. Westberg, Phys. Rev. 114, 1 (1959).

²⁰ L. B. Loeb, Phys. Rev. 94, 227 (1954).

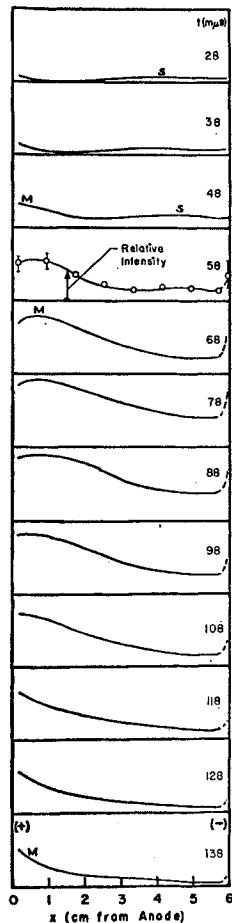


FIG. 21. Cross plots of secondary and main stroke to waning of arc, $r=15.5$ cm, $\delta=6$ cm.

simultaneously throughout the gap. The separation into a primary and a secondary dendrite is very definite in divergent fields, and there are more than one set of such dendrites before each main stroke in the case of longer point-to-plane gaps. At the other extreme, the near parallel plate gap, streamers could not be resolved from the main stroke, at least with the present equipment, for gaps shorter than 1.0 to 1.3 cm.

In the sphere-to-plane gaps for which cross plots were obtained, the main stroke begins its development as the secondary peak nears the cathode. Possibly the secondary produces, or reactivates, a cathode spot which supplies the electrons needed for a rapid rise in current in the ionized channel prepared by the secondary, or perhaps its strongest branch. This increased current produces the further rise in ionization and excitation throughout the gap and the advance of the toe from the anode toward the cathode which characterize the main stroke development, as revealed by the cross-plots of its space wave. In the cases studied, the main stroke, at its height, shows a maximum in intensity near the anode, a trough about 0.5 cm from the cathode, and a rise near the cathode. The oscillograms show that the main stroke toe appears earlier in the 2 mm, or so, adjacent to the

cathode than further out in the gap. In the point-to-plane gaps where the interval between the last primary and the rise of the main stroke may be quite long (1 or 2 μ sec) and where the secondary may not even be observed in the cathode region, it is not clear as to what happens in this interval to initiate the main stroke.

It is difficult to give a criterion for the closeness of approach to the uniform field case, but on the basis of symmetry considerations and discussion in Craggs and Meek,²¹ in which the work of Toepler, Clausnitzer, Meek, and others is cited, it can probably be said that a sphere-to-plane gap is essentially the same as a parallel plate gap when $\delta \leq \delta_K/4$, where δ_K is the gap length at the Toepler discontinuity for a sphere-to-sphere gap with the same value of r . For the two largest spheres used here, with $r=10.2$ and 15.5 cm, $\delta_K/4=1.6$ and 2.0 cm, respectively, while the minimum value of δ at which it was possible to observe streamers is somewhere between 1.0 and 1.3 cm, which value is also greater than half the gap length at which the breakdown surface field begins to increase with decreasing δ between two spheres for the same two values of r . Hence, it appears likely that a dendrite or a streamer would be observed in a parallel plate gap at the sparking threshold for $\delta \geq 1.3$ cm. The actual observation, though difficult, should be attempted.

Whether a dendrite or a streamer could be observed with better resolution in near uniform field gaps much shorter than 1.0 to 1.3 cm is problematical, since the streamer-main stroke interval decreases with decreasing gap length. It is conceivable that the "cathode glow" seen within about 0.5 cm of the cathode and the early rise evident within about 0.2 cm of this electrode in the few cases where this region was studied in some detail, may become the dominant features of the main stroke development in gaps shorter than about 1.0 cm. This would be in agreement with the Kerr cell pictures of Dunnington²² and of White,²³ which show what is doubtless the main stroke developing first at the cathode and in midgap at the sparking threshold in gaps of about 0.4 to 0.6 cm in length between 4-cm diameter spheres. It is important to note that with the Kerr cell one records, as a function of position in the gap, the light output integrated up to the time at which the shutter closes.

The streamer speeds inferred by Loeb,²⁰ those observed by Amin¹⁵ for corona onset streamers, and the speeds given by Saxe and Meek¹² for the leader in gaps with low series resistance lie in a range that begins just below that for the primary streamers, and is well within the range for secondary streamers found in this study. Probably the leader observed by Saxe and Meek is similar to a secondary streamer. Nasser² undoubtedly re-

²¹ J. D. Craggs and J. M. Meek, *Electrical Breakdown of Gases* (Clarendon Press, Oxford, 1953), Chap. 7, p. 311; and *High Voltage Laboratory Technique* (Butterworths Scientific Publications, London, 1954), pp. 224-229.

²² F. G. Dunnington, *Phys. Rev.* **38**, 1535 (1931).

²³ H. J. White, *Phys. Rev.* **46**, 99 (1934), and **49**, 507 (1936).

corded the primary streamer tips, but perhaps with their motion somewhat modified by the nonconducting photographic film in their paths. Whether Raether's¹ cloud track pictures show either a primary or a secondary is difficult to determine, since he was working with uniform field geometry and highly overvolted impulse breakdown. It is possible that he observed secondaries of high speed under these conditions.

ACKNOWLEDGMENTS

The authors wish to express their gratitude to the Office of Naval Research and the Research Corporation for their support of this project; to Dr. Harry J. White, Dr. Norman Seaton, Dr. R. G. Westberg, and Dr. Peter Wagner for many stimulating and helpful discussions; and to many others, too numerous to name, for their help.

PHYSICAL REVIEW

VOLUME 123, NUMBER 1

JULY 1, 1961

Streamer Mechanism in Filamentary Spark Breakdown in Argon by Fast Photomultiplier Techniques*

L. B. LOEB, R. G. WESTBERG,[†] AND H. C. HUANG[‡]*Department of Physics, University of California, Berkeley, California*

(Received June 1, 1960; revised manuscript received January 10, 1961)

Using techniques developed by Hudson on air and reported in the preceding paper, the phenomena were studied in Linde's spectroscopically pure grade Ar gas admitted to a system using Alpert vacuum techniques, and on that gas further purified by gas cataphoresis. Study was made in a point-to-plane gap with a 2.36-mm hemispherically capped cylinder opposite a 3-cm distant thin out-gassed Ni plane in the pressure range from 300 mm to 50 mm. For the spectroscopically pure grade Ar, transition from a positive point corona through a fine filamentary spark to an incipient arc breakdown on a time scale of 10^{-7} sec down to 100 mm pressure proceeds by movement of primary and secondary streamers progressing from anode to cathode at slower speeds

and lower luminous intensities than air at 760 mm. Unlike the case for air, the main stroke in Ar appears to move from anode towards the cathode. At 50 mm a somewhat diffuse spark channel did not reveal any streamer-like progression but the time scale was still in the 10^{-7} -sec range. One percent air in Ar at 60 mm restored streamers. Purified Ar at 240 mm revealed a 2-mm wide diffuse channel breakdown occurring across the whole gap by a process unknown with a rise time of several microseconds and sustained luminosity for tens of μ sec with no indication of streamers. This demonstrates the necessity of adequate photoionizable impurities in Ar for the development of the filamentary streamer spark transition.

INTRODUCTION

EVIDENCE has been presented by Hudson¹ for the transition from an antecedent positive point corona or glow discharge of low order to an incipient transient arc through the filamentary spark in consequence of a sequence of luminous streamers or dendrites starting from the anode and crossing to the cathode. These streamer-like luminosities taken from oscillograms of the light pulses crossing the slit at various distances from the anode may be depicted as luminous space waves moving from anode to cathode at various times by means of cross plots. This enables the velocities of the different portions of these waves to be evaluated. Quite complete data are thus obtained for the longer gaps with regions of low field where velocities are low. As one progresses to gaps with more uniform and higher fields and especially for the shorter gaps, velocities become so high and times so short in air that the complete

analysis is no longer possible within the resolving time of the oscilloscopes. However, even then the presence of some of the pulses as they approach the cathode strongly suggests that the anode streamer mechanism persists, a matter consistent with the remarkably short time scales of breakdown which preclude any Townsend-like mechanism.

As the streamer mechanism was initially invoked by Raether² and Loeb and Meek,² it was believed that when an electron avalanche reached a magnitude to yield an adequate positive ion space-charge density at the anode, together with intense photoionization in close proximity to the space charge, a single positive streamer progressed across the gap from anode to cathode at high speed. From this point on, Raether working with overvolted gaps considered that the conducting channel was established and that the arc materialized by steady but fast increase in current. Loeb and Meek, in analogy to the lightning stroke and Allibone and Meek's³ observations on long sparks, believed that the heavy

* This study has been supported by the Office of Naval Research, the Research Corporation, and a National Research Council Fellowship.

[†] Now at Philips Laboratories, Irvington-on-Hudson, New York.

[‡] Now at University of Malaya at Kuala Lumpur, Malaya.

¹ G. G. Hudson, doctoral dissertation, University of California, 1957 (unpublished); G. G. Hudson and L. B. Loeb, preceding paper [Phys. Rev. **123**, 29 (1961)].

² L. B. Loeb, in *Encyclopedia of Physics*, edited by S. Flügge (Springer-Verlag, Berlin, 1956), Vol. 22, p. 484 ff; H. Raether, *Ergeb. exakt. Naturw.* **22**, 736 (1949).

³ T. E. Allibone and J. M. Meek, *Proc. Roy. Soc. (London)* **A166**, 97 (1938), **A169**, 246 (1938). F. F. Saxe, J. M. Meek, and T. E. Allibone, *Nature* **162**, 263 (1948).

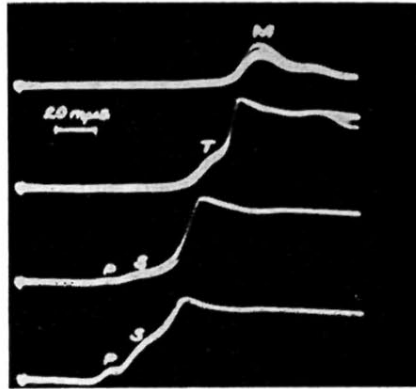


FIG. 10. Near the cathode the main stroke and tertiary, secondary, and primary pulses appear in successive frames as the PM slit width increases from top to bottom. The origin of time is the same for all frames. Sweep rate = $20 \text{ m}\mu\text{sec/cm}$. $r = 1.9 \text{ cm}$, $\delta = 1.5 \text{ cm}$.

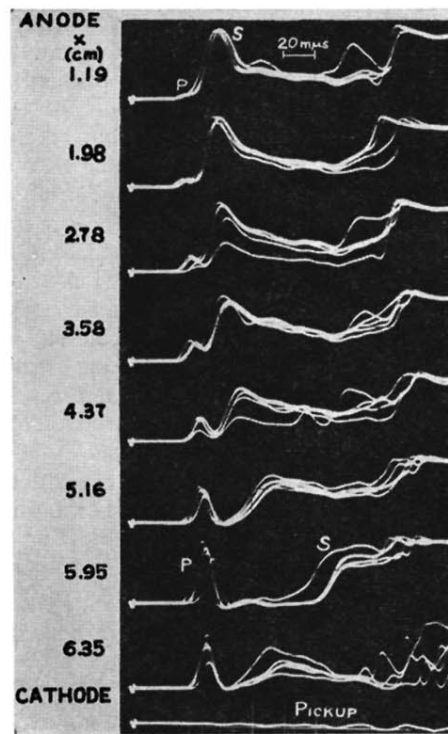


FIG. 11. The development of the single primary-secondary dendrite set preceding each main stroke for $r=6.35$ cm and $\delta=6.4$ cm. The main stroke overloads the CRO, but its rise appears at the right.

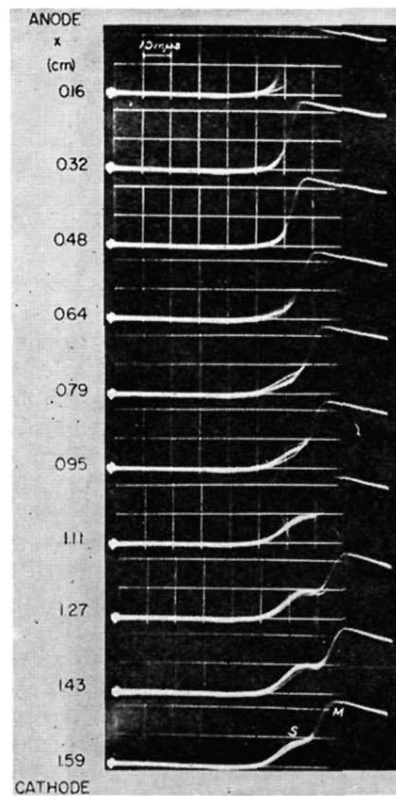


FIG. 14. CRO traces, for nearly parallel plate geometry, showing a streamer, or dendrite, in the cathode half of the gap, and the main stroke toe. (Its peak overloads the CRO.) $r=15.5$ cm, $\delta=1.65$ cm.

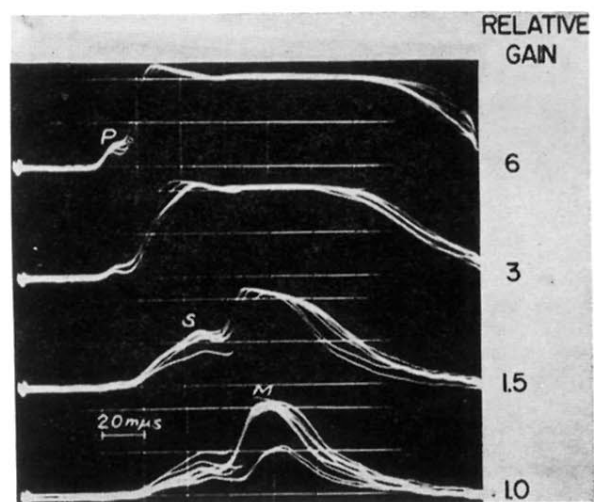


FIG. 16. Oscillograms on fast sweep at varying gains near cathode for $r=15.5$ cm and $\delta=6$ cm, showing primary, secondary, and main stroke. The origin of time was fixed as only the PM slit was varied.

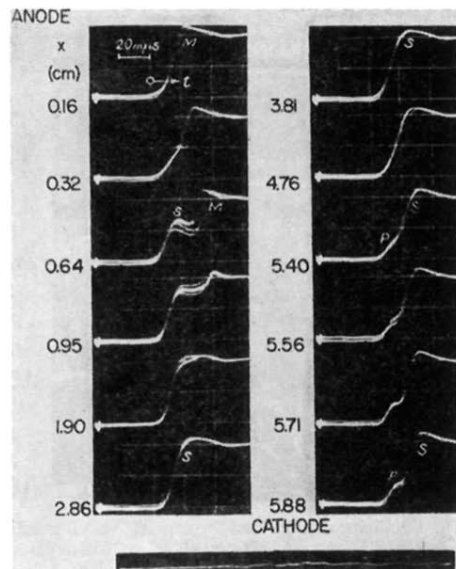


FIG. 17. CRO traces showing the primary (near the cathode), the secondary (with CRO overloaded for $x > 0.95$ cm), and the toe of the main stroke (for $x \leq 0.95$ cm). $r = 15.5$ cm, $\delta = 6$ cm. Electrical pickup on trace below.

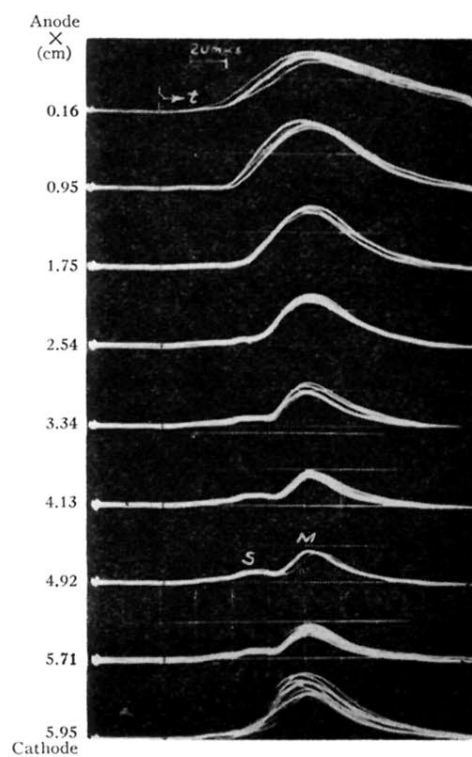


FIG. 18. Oscillograms showing secondary streamer and main stroke for $r=15.5$ cm, $\delta=6.0$ cm.

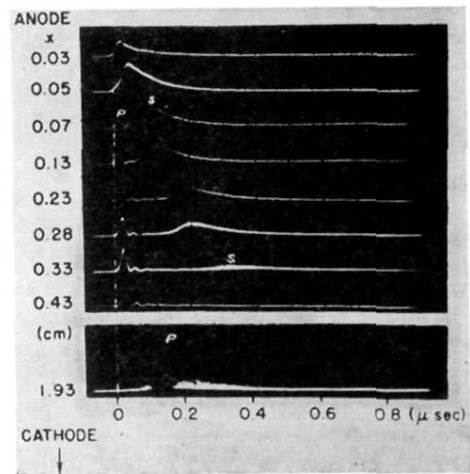
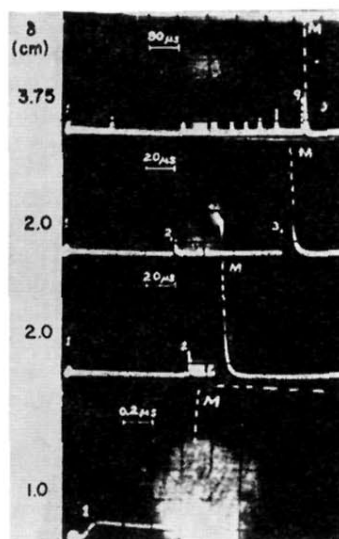


FIG. 2. CRO traces showing primary and secondary dendrites below breakdown for a needle point with $\delta=5$ cm.

FIG. 3. Oscillograms, taken at slow sweep speeds, of the succession of dendrite sets preceding a single main stroke for several gap lengths with the same point (tip $r=0.04$ cm). Primaries and secondaries are unresolved.



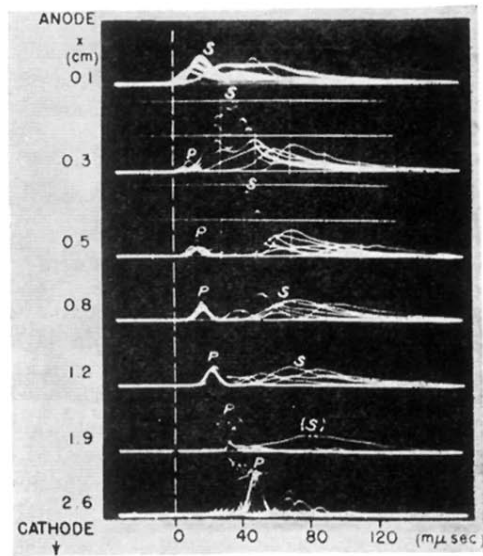


FIG. 4. Superimposed traces at varying x of the seven, or so, primary-secondary dendrite sets preceding a single main stroke. (Two main strokes at $x=2.6$ cm.) $r=0.04$ cm, $\delta=3.0$ cm.

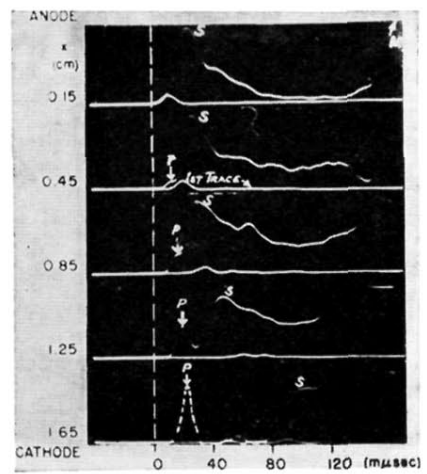


FIG. 5. Oscillograms of the two dendrite sets preceding the main stroke, the rise of which appears at the right on the second trace. $r=0.1$ cm, $\delta=1.7$ cm.

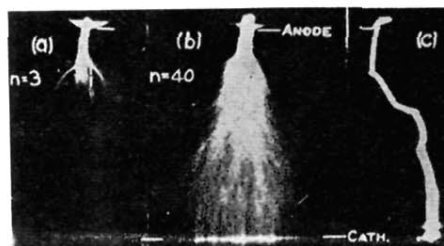


FIG. 6. Still photograph under unique geometry, showing streamers just at breakdown and resulting spark at right.

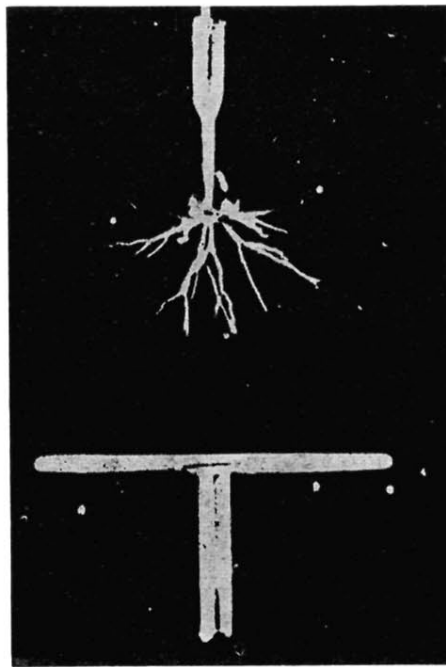


FIG. 7. An early cloud chamber photograph of branched secondary streamers in interrupted point-to-plane impulse breakdown by Gorrill.